


Meropenem inhibits *Acinetobacter baumannii* biofilm formation by downregulating *pgaA* gene expression

Mir Mahdi Najafi^{1*} 

¹Chemical Injuries Research Center, Systems Biology and Poisonings Institute, Baqiyatallah University of Medical Sciences, Tehran, Iran

ARTICLE INFO

Original Article

Keywords: *Acinetobacter baumannii*, atomic force microscope, Biofilm, *PgaA*, RT-PCR, Antibiotic resistance

Received: 29 Sep. 2021

Received in revised form: 04 Jul. 2023

Accepted: 11 Jul. 2023

DOI: 10.61186/JoMMID.11.2.86

*Correspondence

Email: mirmahdinajafi@gmail.com

Tel: +982188655366

Fax: +982188202521

© The Author(s)



ABSTRACT

Introduction: *Acinetobacter baumannii* is the cause of nosocomial infections, primarily in intensive care units. The *pgaA* gene plays an essential role in biofilm formation, making it a promising target for developing new strategies to tackle *A. baumannii* infections. This study investigated the meropenem effect on *pgaA* gene expression and biofilm formation in *A. baumannii*. **Methods:** Over five months, 50 urine samples were taken from patients receiving medical care in the intensive care unit, of which 20 *A. baumannii* isolates were detected. Antibiotic susceptibility was determined with meropenem, imipenem, trimethoprim/sulfamethoxazole, ceftazidime, ciprofloxacin, tetracycline, amikacin, as well as gentamicin disks by the Kirby-Bauer method. The minimum inhibitory concentration (MIC) of meropenem was determined using the microdilution method. Biofilm formation was investigated through the tissue culture plate (TCP) technique and imaged using an atomic force microscope (AFM). Reverse Transcriptase Polymerase Chain Reaction (RT-PCR) determined the expression level of the *pgaA* gene. **Results:** Antibiotic susceptibility testing revealed that all *A. baumannii* isolates were resistant to meropenem, imipenem, ciprofloxacin, and amikacin, and 71.42% were resistant to tetracycline. The MIC for meropenem could not be determined for isolates. Meropenem prevented biofilm formation in more than 70% of the isolates, and AFM imaging revealed thin biofilms. The RT-PCR showed that exposure to meropenem significantly decreased the *pgaA* expression gene in over 95% of the isolates ($P < 0.0001$). **Conclusion:** Meropenem inhibited biofilm formation in most *A. baumannii* isolates by downregulating the *pgaA* expression, suggesting a potential role in preventing *A. baumannii* infections by reducing biofilm formation.

INTRODUCTION

Acinetobacter baumannii is a Gram-negative, aerobic, non-fermenting opportunistic pathogen in hospital intensive care units (ICUs) [1-3]. This bacterium can cause a wide range of infections, including ventilator-associated pneumonia (VAP), bacteremia, skin and soft tissue infections (SSTI), post-traumatic and urinary tract infections (UTIs), endophthalmitis, keratitis, meningitis, and, occasionally, endocarditis [4]. The mortality rate among vulnerable patients can reach 60%, while the reported mortality rates in hospitals and ICUs range from 23% to 28% and 10% to 43%, respectively [5, 6]. The Infectious Diseases Society of America (IDSA) has

defined *A. baumannii* as one of the top seven pathogens threatening health and treatment centers [7]. The rapid acquisition of antibiotic-resistant genes and high environmental resistance levels of this pathogen makes controlling and eradicating it challenging [2, 8]. The expression levels of several pathogenic genes, including genes related to quasi-sensing systems and those involved in biofilm formation, are among the essential factors contributing to bacterial resistance, longevity, and survival in the host [9, 10].

Meropenem is a broad-spectrum antibiotic belonging to the β -lactam and carbapenem groups [11]. Carbapenems

are currently the preferred drugs for treating *A. baumannii* infections. Resistance to this antibiotic poses a significant concern to public health authorities and limits treatment options. This resistance can result from the horizontal transfer of resistance genes and variations in the expression levels of intrinsic genes, such as β -lactamases (*OXA23*, *OXA24*, *OXA51*, and *OXA58*), *AmpC*, efflux pumps, integrons, and Metallo beta-lactamases (IMP, VIM, SIM, GIM, and NDM) [12-14]. *A. baumannii* bacteria can efficiently survive in the environment by forming biofilms, which allow them to adhere to surfaces such as medical equipment and remain viable in the presence of antibiotics and antimicrobial agents [15, 16]. The *csuA/BABCDE* system is one of the factors contributing to biofilm formation in *A. baumannii*. The CSU operon comprises six genes, *csuA/BABCDE*, which encode the chaperone-usher system and are involved in biofilm formation on non-living surfaces. The expression of *csuA/BABCDE* triggers both biofilm and pili production, and the inactivation of *csuE* halts the production of pili and biofilm [17]. The expression of *csuA/BABCD* is regulated by a system comprising the sensor kinase BfmS and the response regulator BfmR. Inactivation of BfmR results in the loss of *csuA/BABCDE* expression and inhibits biofilm formation on plastic surfaces in cells cultured in enriched media. Inactivation of BfmS reduces adherence to eukaryotic cells and decreases but does not entirely inhibit biofilm formation on abiotic surfaces in *A. baumannii* ATCC 17978 [18, 19].

The protein OmpA, encoded by the *ompA* gene, has been found to play a crucial role in forming biofilms. This trimeric porin and outer membrane protein acts as a pore for dispersion and a factor for bacterial attachment to plastic surfaces, epithelial cells, and *Candida albicans* filaments. It is also a potential virulence factor and has been implicated in causing epithelial cell death, early-onset apoptosis, delayed-onset necrosis of dendritic cells, cell death through mitochondrial targeting, and induction of reactive oxygen species (ROS) production [19]. The biofilm-associated protein (Bap) is also involved in developing biofilms on various layers. This protein enhances bacterial adhesion to human bronchial epithelial cells and neonatal keratinocytes by increasing the hydrophobicity of the bacterial cell surface. It is necessary to form a three-dimensional tower structure and water channels on the surfaces of medical equipment, including polypropylene, polystyrene, and titanium. Another factor identified in *A. baumannii* ATCC 17978 is the PglC protein, which can form biofilms, increasing their volume and density [18, 20]. The development and maturation of *A. baumannii* biofilm critically depend on the PNAG protein encoded by the four *pgaABCD* genes. Modifying or inactivating these genes can impact bacterial biofilm formation [21, 22].

The atomic force microscope (AFM), a scanning probe microscope (SPM), can achieve atomic spatial resolution for conductive, non-conductive, and biological samples,

including biomolecules, DNA, proteins, bacteria, and bacterial biofilms [23, 24].

Controlling hospital-acquired infections (HAIs) is one of the most critical challenges facing health and treatment systems today. Given that *A. baumannii* is a highly opportunistic pathogen that readily forms biofilms in hospital settings, this study employed AFM to investigate the structure of *A. baumannii* biofilms and determined the expression level of *pgaA* following exposure to meropenem.

MATERIAL AND METHODS

Isolation and identification of microbial strains.

Between January and May 2020, 50 urine samples were collected from patients hospitalized in the Intensive Care Unit (ICU) at Loghman Hakim Hospital in Tehran, Iran. The samples were cultured using standard laboratory techniques. Each sample was cultured individually on blood agar and MacConkey agar media (Merck, Germany), then transferred to the laboratory and incubated at 37 °C for 24-48 h. The Giemsa staining solution was prepared using a commercial kit (Kalazist Co., Iran). Phenotypic tests, including oxidase, catalase, and citrate utilization [25], were used to identify 20 isolates of *A. baumannii*. This study was approved by the Iran National Committee for Ethics in Biomedical Research (approval No. IR.IAU.VARAMIN.REC.1397.002).

Antibiotic resistance patterns. The Kirby-Bauer method was used to perform antibiograms. Broth bacteria cultures with turbidity equivalent to a 0.5 McFarland standard were plated on Mueller-Hinton agar (Merck, Germany) and incubated for 24 h. Sterile forceps were used to place antibiotic disks on the cultured bacteria. Inhibition zone diameters were measured after incubating the plates at 37 °C for 24 h, and isolates were classified as susceptible (S), resistant (R), or intermediate (I) (Table 1). Moreover, a chart showing the percentage of *A. baumannii* isolates resistant to each antibiotic was created for antibiotics described [26, 27]. The positive control for the assays was the standard *A. baumannii* ATCC 19606 strain.

Meropenem minimum inhibitory concentration

(MIC). Meropenem dilutions ranging from 1 to 512 $\mu\text{g/mL}$ (Padtan Teb Co., Iran) were prepared using broth microdilution, with ten consecutive dilutions. Muller-Hinton broth (Merck, Germany) was prepared, and 100 μl was dispensed into wells of a 96-well plate. A 100 μl volume of meropenem solution was added to the first row, and serial dilutions were prepared in the remaining rows. To achieve a concentration of 10^6 CFU/mL, a 1/100 dilution was made from the microbial suspension with turbidity equivalent to a 0.5 McFarland standard, and 100 μl of this dilution was added to each well. The MIC was determined as the lowest concentration of meropenem that inhibited visible bacterial growth after incubating the plate for 24 hours at 37 °C [27, 28]. The optical density at

620 nm for all wells was measured using an ELISA Reader Citation 3 instrument (Bio Tek Instruments Inc., USA) to minimize optical illusions during the experiment. Positive control wells containing culture medium and

bacteria and negative control wells containing culture medium and meropenem solution were included to ensure the quality of the investigation.

Table 1. The antibiotic resistance patterns of *A. baumannii* isolates were determined by measuring the zone of inhibition (CLSI 2018).

Antibiotics	Symbol	Sisk content (μg)	S*	I*	R*
Meropenem	MEN	10	≥ 18	15-17	≤ 14
Imipenem	IPM	10	≥ 22	19-21	≤ 18
Trimethoprim-sulfamethoxazole	SXT	1.25/23.75	≥ 16	11-15	≤ 10
Ceftazidime	CAZ	30	≥ 18	15-17	≤ 14
Ciprofloxacin	CP	5	≥ 21	16-20	≤ 15
Tetracycline	TE	30	≥ 15	12-14	≤ 11
Amikacin	AN	30	≥ 17	15-16	≤ 14
Gentamicin	GM	10	≥ 15	13-14	≤ 12

* Sensitive, Intermediate, Resistant

Biofilm formation. To assess *A. baumannii* biofilm formation, the tissue culture plate (TCP) method was used with and without meropenem, which is considered the gold standard [29]. To assess the effect of meropenem, *A. baumannii* isolates were initially cultured on trypticase soy agar (Merck, Germany) supplemented with 2% glucose. After 24 hours of incubation at 37 °C, bacterial suspensions with a turbidity equivalent to a 0.5 McFarland standard were prepared in trypticase soy broth (TSB) (Merck, Germany), and 200 μL of each isolate's suspension was added to three wells of a 96-well polystyrene plate. The plates were incubated at 37 °C, washed twice with phosphate-buffered saline (PBS, pH 7) (Sigma Aldrich Corp., USA), fixed with 95% methanol for 15 minutes, and stained with 1% crystal violet for 5 minutes. The plates were subsequently emptied and rinsed with sterile distilled water. Each well was treated with 100 μL of 33% acetic acid, and the absorbance was measured at 570 nm using an ELISA Reader Citation 3 instrument [30]. To assess the impact of meropenem on biofilm formation, the *A. baumannii* suspension was treated with a 1 mg/mL meropenem solution and then incubated at 37 °C for 24 h. The remaining steps were identical to those performed without the addition of meropenem. The ability of isolates to form biofilms was determined based on the OD cut-off value, which was calculated as the mean absorbance value of the negative control plus three standard deviations ($\text{ODc} = \text{M} + 3\text{SD}$) [31]. Each sample was tested in triplicate, with *A. baumannii* ATCC 19606 used as the positive control and 200 μL of TSB containing 2% glucose as the negative control.

Phenotypic analysis of biofilm formation. The formation of bacterial biofilms was assessed using the

tissue culture plate (TCP) method, with and without the addition of meropenem (1 mg/mL). The biofilms were fixed with 2.5% glutaraldehyde for an hour and then dehydrated sequentially using increasing concentrations of methanol (70%, 75%, 80%, 85%, 90%, and 95%) for 10 min each. Subsequently, the biofilms were imaged using an atomic force microscope (AFM) (Olympus, Tokyo, Japan), and the resulting images were compared [32-37].

Molecular Analysis of *pgaA* Expression by RT-PCR.

To extract RNA from *A. baumannii* isolates, a commercial RNA extraction kit (GeneAll Biotechnology Co. Ltd, Korea) was used. The RNA yield was quantified by measuring the absorbance at 260 nm using a Nanodrop instrument, and the purity was determined by calculating the OD 260/280 ratio. The RNA was utilized to synthesize complementary DNA (cDNA). To synthesize cDNA, 1000 ng of RNA was treated with DNase and processed according to the manufacturer's instructions (GeneAll Biotechnology Co. Ltd, Korea). The primers utilized for amplifying *16S rRNA* and *pgaA* are presented in Table 2 [38, 39]. Each 25 μL reaction mixture comprised 8.5 μL sterile double-distilled water, 12.5 μL 2X SYBR Green master mix (Ampliqon, Denmark), 3 μL of each forward and reverse primer (5 pmol), and 1 μL cDNA. Amplification was performed using a thermocycler (StepOnePlus, ABI Co. USA) with an initial denaturation step at 95 °C for 15 min, followed by 40 cycles of denaturation at 95 °C for 15 s, and annealing and amplification at 60 °C for 1 min. Each sample was tested in duplicate.

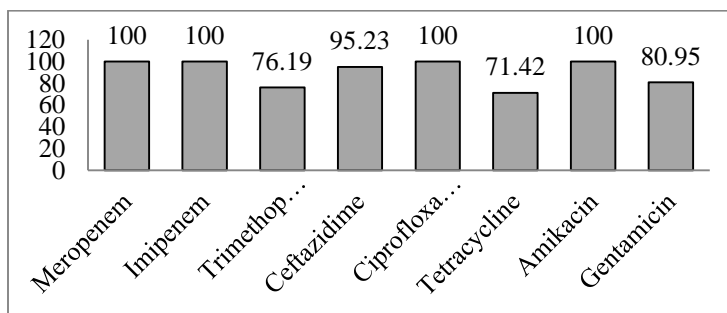
Table 2. The primers used for the amplification of *16S rRNA* and *pgaA* genes

Gene	Primer sequences (5'→3')	Amplicon size
<i>pgaA</i>	GCCGACGGTCGCGATAC	126 bp
	ATGCACATCACAAAACGGTACT	
<i>16S rRNA</i>	ACTCCTACGGGAGGCAGCAGT	140 bp
	TATTACCGCGGCTGCTGGC	

Statistical analysis. The data were analyzed with GraphPad Prism 5, and the expression levels of these genes in the treated strains were compared to those in the control strains using the $2^{-\Delta\Delta Ct}$ method. The significance level of the data was determined to be $P \leq 0.05$ utilizing a t-test.

RESULTS

Antibiotic resistance. Resistance to several antibiotics was observed in the *A. baumannii* isolates, with rates of 76.19% for trimethoprim-sulfamethoxazole, 95.23% for ceftazidime, 71.42% for tetracycline, and 80.95% for gentamicin. All isolates exhibited resistance to meropenem, imipenem, ciprofloxacin, amikacin, and other antibiotics (Fig. 1).

**Fig. 1.** Resistance rates of *A. baumannii* isolates to the eight antibiotics used in this study.

Meropenem MIC. No MIC was obtained for isolates at concentrations $>512 \mu\text{g/mL}$, indicating 100% resistance according to the CLSI 2018 standard.

Biofilm formation in the absence of meropenem treatment. The OD of the negative control wells was calculated to be 0.213 using the formula $(0.156 + 3 \times 0.019)$. The isolates were classified into two groups based on their biofilm formation ability, and of the 20 isolates tested, 18, including *A. baumannii* ATCC 19606, exhibited strong biofilm formation ability. At the same time, two had moderate biofilm formation ability. All isolates exhibited at least moderate biofilm formation ability, with none showing a weak power or failing to produce biofilms (Table 3). A photograph of the biofilm formation assay plate is presented in Figure 2. Figure 3 illustrates the percentage of biofilm formation for each

isolate measured using the culture plate (TCP) method under the influence of meropenem.

Biofilm formation in the presence of meropenem treatment. The OD of the negative control wells was calculated to be 0.2426 using the formula $(0.1787 + 3 \times 0.0213)$. Based on biofilm formation ability in the presence of meropenem, the isolates were classified into three groups; of the 20 isolates, 15, including *A. baumannii* ATCC 19606, did not exhibit biofilm formation in the presence of meropenem, three had weak biofilm formation ability, and two had moderate biofilm formation ability (Table 4). The biofilm formation assay plate in the presence of meropenem is illustrated in Figure 4. The percentage of biofilm formation for each isolate was determined using the TCP method (Fig. 5).

Table 3. Classification of isolates by biofilm formation ability in the absence of meropenem treatment

Average OD value	Biofilm production	Observed OD	In this study
$\text{OD} > 4\text{ODc}$	Strongly adherent	$\text{OD} > 0.852$	Strongly adherent
$2\text{ODc} < \text{OD} \leq 4\text{ODc}$	Moderately adherent	$0.426 < \text{OD} \leq 0.852$	Moderately adherent
$\text{ODc} < \text{OD} \leq 2\text{ODc}$	Weakly adherent	-	-
$\text{OD} \leq \text{ODc}$	Non-adherent	-	-

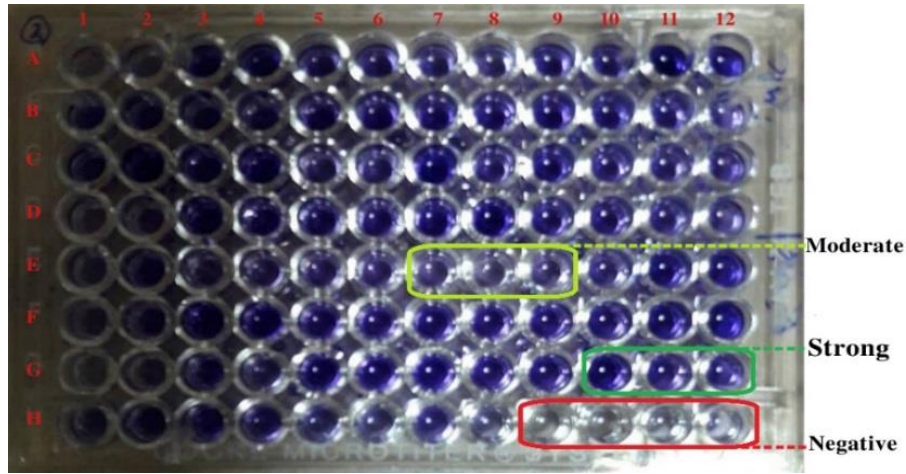


Fig. 2. Biofilm formation of *A. baumannii* isolates without meropenem treatment.

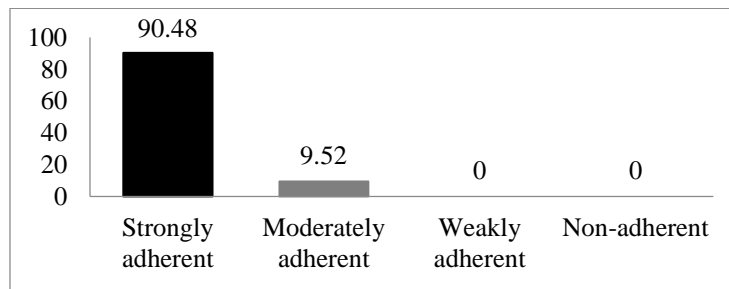


Fig. 3. Biofilm formation ability of *A. baumannii* isolates without meropenem.

Table 4. Biofilm formation ability of the *A. baumannii* isolates in the presence of meropenem.

Average OD value	Biofilm production	Observed OD	In this study
OD>4ODc	Strongly adherent	-	-
2ODc<OD≤4ODc	Moderately adherent	0.485<OD≤0.970	Moderately adherent
ODc<OD≤2ODc	Weakly adherent	0.242<OD≤0.485	Weakly adherent
OD≤ODc	Non-adherent	OD≤0.242	Non-adherent

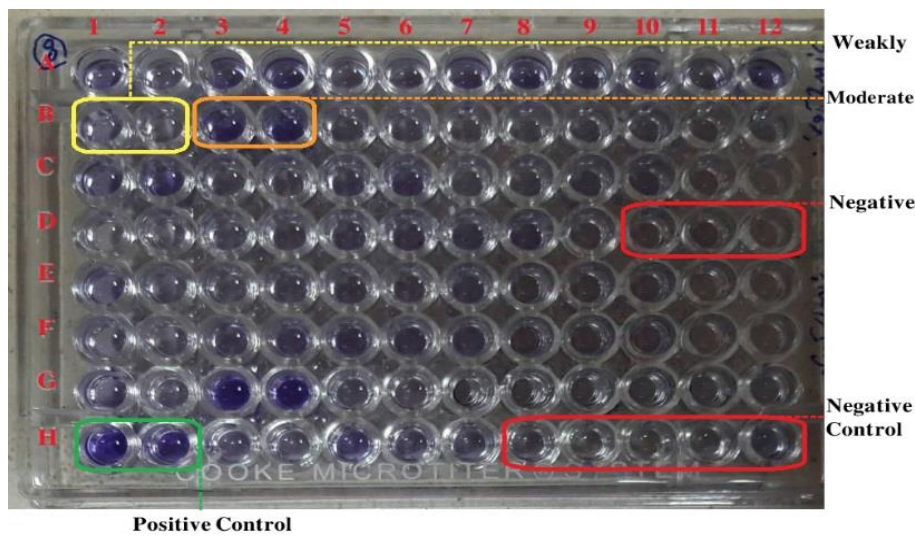


Fig. 4. Biofilm formation ability *A. baumannii* of isolates in the presence of meropenem.

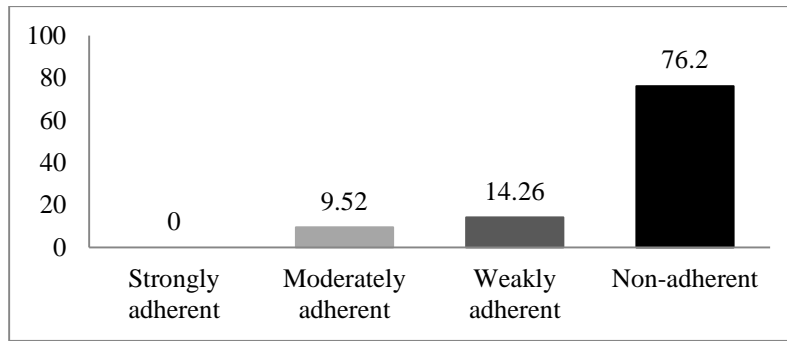


Fig. 5. Biofilm formation ability of *A. baumannii* of isolates in the presence of meropenem.

AFM images. Before meropenem treatment, AFM images revealed dense masses of coccus-like layers stacked on each other, with thicknesses ranging from 0 to 3 μm . Images 3A, 3B, 3D, and 3E in Figure 6 indicate that the bacteria were active and capable of forming biofilms.

However, after adding meropenem, the distance between cells and the density of biofilm formation in the coccus-like population decreased by approximately 0 to 900 nm. Images 3C and 3F in Figure 6 demonstrate that meropenem substantially affected biofilm formation.

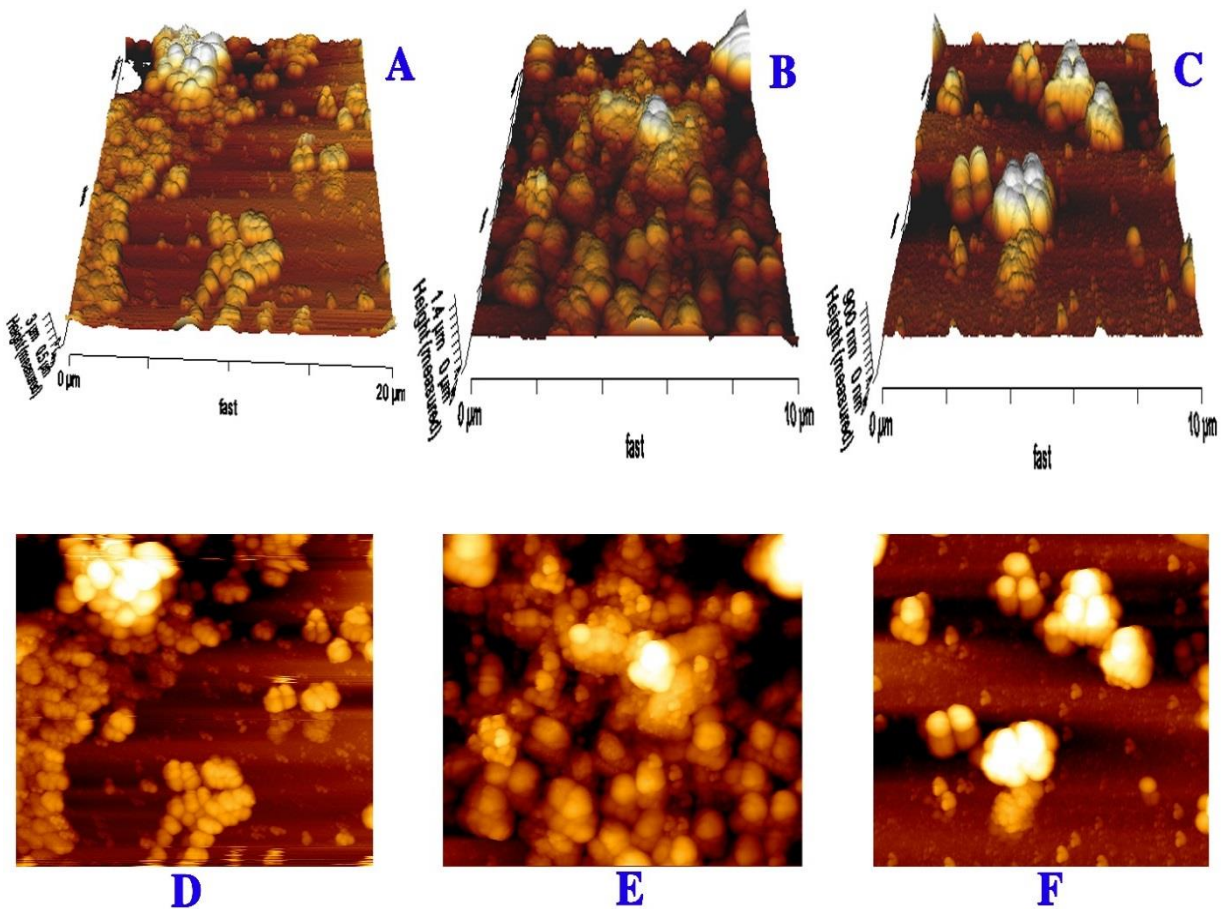


Fig. 6. AFM Images of *A. baumannii* biofilm formation before (images A, B, D, and E) and after (images C and F) meropenem treatment.

***pgaA* expression.** After the addition of meropenem, the expression levels of *pgaA* in *A. baumannii* samples decreased by over 95% (Fig. 7), which was significantly

different from samples without meropenem ($P < 0.0001$) (Fig. 8).

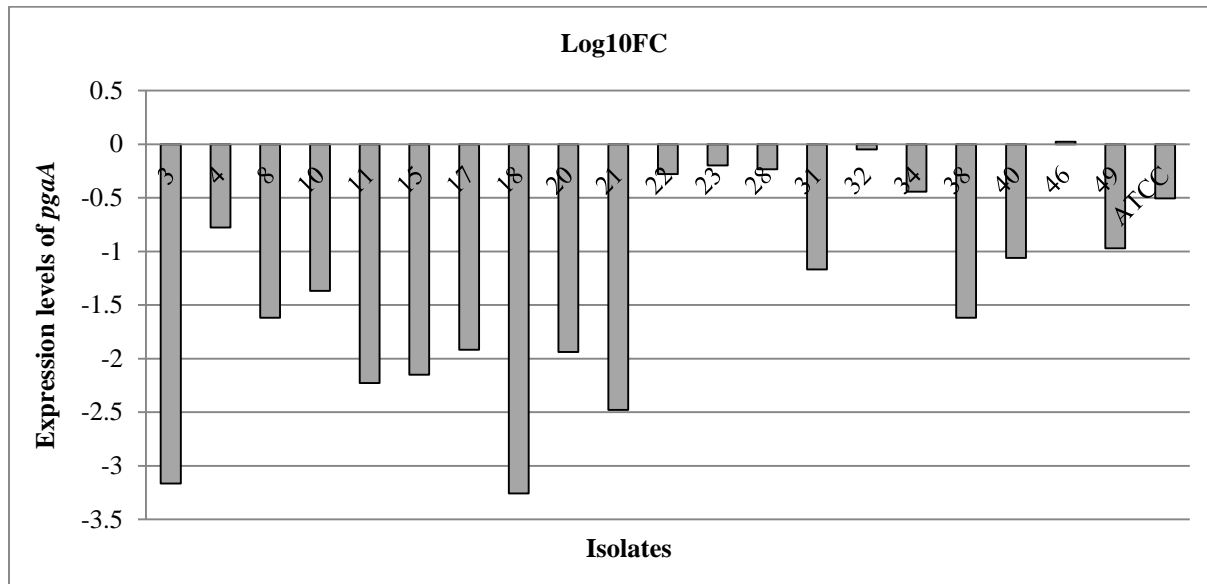


Fig. 7. Expression levels of *pgaA* in *A. baumannii* isolates after adding meropenem to cultures. P value <0.0001

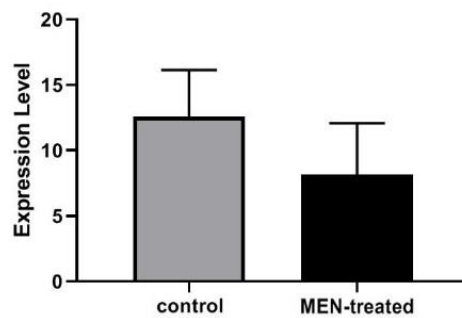


Fig. 8. Statistical significance of data based on t-test (P -value)

DISCUSSION

Healthcare-associated infections (HAIs) caused by opportunistic pathogens have increased over the past years. This trend is expected to persist as the number of hospitals grows, creating significant challenges and costs for people and governments [40, 41]. According to the Centers for Disease Control and Prevention (CDC), the most commonly reported healthcare-associated infections (HAIs) are urinary tract infections (42%), surgical wound infections (24%), lower respiratory tract infections (15-20%), and bloodstream infections (5-10%). Biofilm-forming bacteria are responsible for 80% of urinary tract infections [42]. Studying the factors, mechanisms, and genes involved in *A. baumannii* biofilm formation during urinary tract infections can help identify effective treatment and prevention strategies to mitigate the risk of recurrent infections and associated urinary complications.

Carbapenem-resistant *A. baumannii* infections present a significant challenge in antibiotic treatment. The inappropriate use of antibiotics to treat bacterial infections is one of the primary factors contributing to the development and spread of antibiotic resistance. This

phenomenon leads to a shortened effective lifespan of antibiotics and raises concerns over the unavailability of new antibiotics [43]. A study reported that 33.3% of *A. baumannii* isolates were resistant to meropenem, and 44.5% were resistant to ciprofloxacin. In addition, 45.5% of *Pseudomonas aeruginosa* isolates were resistant to meropenem, and 36.4% were resistant to ciprofloxacin [44]. Similar reports showed that all *A. baumannii* isolates tested were multidrug-resistant [45], consistent with our results. Our study found that all the isolates were resistant to clinically essential β -lactam antibiotics, including meropenem and imipenem, consistent with a previous report [46]. Ghajavand *et al.* (2015) found that 93% of *A. baumannii* isolates were resistant to both imipenem and meropenem, 86% were resistant to ceftazidime, and all isolates were resistant to ciprofloxacin [25]. Moradi and Hashemi (2015) reported that the prevalence of this resistance increased from 51.1% to 64.3% between 2001 and 2007 and from 76.5% to 81.5% between 2012 and 2013. These reports indicate that antibiotic resistance in *A. baumannii* isolates has increased in Iran and globally in recent years [47]. Beganovic and Luther (2019)

investigated the impact of several antibiotics on biofilm formation in different *Acinetobacter* species. The biofilms are classified as weakly, moderately, or strongly adherent. Minocycline and polymyxin B were found to be the most effective antibiotics against *A. baumannii*, with the ability to prevent biofilm formation in most isolates [48]. The results of this study, as well as those of Wang and Kuo (2016), showed that meropenem significantly disrupted the structure of *A. baumannii* biofilms [49]. The degradation was observed with prolonged or high-dose use of imipenem [50]. Both the present study and the similar study demonstrated that the formation of biofilm was significantly lower in meropenem-sensitive isolates compared to meropenem-resistant ones ($P < 0.0001$) [51]. The present study and two similar ones [52, 53] have shown that atomic force microscopy (AFM) is a valuable tool for visualizing biofilm structure and observing biofilm formation in bacteria. Hatami (2018) observed that 80% of the isolates were resistant to imipenem, and the expression levels of the *pgaA* and *abaI* genes were 58% and 18%, respectively [54]. Our findings were consistent with those of Choi and Slamti (2009), which found that all studied isolates had *pgaA*. However, they also identified ten isolates that expressed PNAG using a western blotting procedure [21].

The *pgaA* gene is an essential factor in the biofilm formation of *A. baumannii*. The AFM images showed a significant reduction in the biofilm formation of this bacterial species in response to meropenem. The use of antibiotics without a standard protocol for prescribing can lead to irreparable epidemics of *A. baumannii*. To prevent the spread of *A. baumannii* epidemics, adherence to established academic principles when prescribing antibiotics such as meropenem is recommended by the current research. One of the most significant limitations of the study was the COVID-19 epidemic in Iran, which led to the allocation of all beds in the hospital's intensive care unit for patients with respiratory problems. Another major challenge was preventing the contamination of urine samples with other microorganisms. Due to urinary catheters in most patients hospitalized in the intensive care unit, their urine remained in the environment for an extended period, making it impossible to include them in the study. Furthermore, the study was limited by its relatively short duration of five months. Future research should investigate other potential factors and genes contributing to biofilm formation, including purines, the cell wall capsule and lipopolysaccharide, additional enzymes, and the iron absorption system.

ACKNOWLEDGMENT

The author thanks the Clinical Research Development Unit at Loghman Hakim Hospital and the Comprehensive Research Laboratory at Shahid Beheshti University of Medical Sciences for their support and cooperation during this research. The research received no funding from public, commercial, or not-for-profit agencies.

CONFLICT OF INTEREST

The authors declare that there are no conflicts of interest associated with this manuscript.

REFERENCES

- Brooks GF, Carroll KC, Butel JS, Morse SA. Jawetz, Melnick & Adelberg's Medical Microbiology. 24th ed. USA: McGraw-Hill; 2007. 273-5.
- Huang LY, Chen TL, Lu PL, Tsai CA, Cho WL, Chang FY, et al. Dissemination of multidrug-resistant, class 1 integron-carrying *Acinetobacter baumannii* isolates in Taiwan. Clin Microbiol Infect. 2008; 14 (11): 1010-9.
- Cisneros JM, Rodríguez-Baño J. Nosocomial bacteremia due to *Acinetobacter baumannii*: epidemiology, clinical features and treatment. Clin Microbiol Infect. 2002; 8 (11): 687-93.
- O'Shea MK. *Acinetobacter* in modern warfare. Int J Antimicrob Agents. 2012; 39 (5): 363-75.
- Abdi SN, Ghotaslou R, Ganbarov K, Mobed A, Tanomand A, Yousefi M, et al. *Acinetobacter baumannii* Efflux Pumps and Antibiotic Resistance. Infect Drug Resist. 2020; 13: 423-34.
- Nasiri MJ, Zamani S, Fardsanei F, Arshadi M, Bigverdi R, Hajikhani B, et al. Prevalence and Mechanisms of Carbapenem Resistance in *Acinetobacter baumannii*: A Comprehensive Systematic Review of Cross-Sectional Studies from Iran. Microb Drug Resist. 2020; 26 (3): 270-83.
- Talbot GH, Bradley J, Edwards JE, Jr., Gilbert D, Scheld M, Bartlett JG. Bad bugs need drugs: an update on the development pipeline from the Antimicrobial Availability Task Force of the Infectious Diseases Society of America. Clin Infect Dis. 2006; 42 (5): 657-68.
- Fournier PE, Richet H, Weinstein RA. The Epidemiology and Control of *Acinetobacter baumannii* in Health Care Facilities. Clin Infect Dis. 2006; 42 (5): 692-9.
- Zarrilli R. *Acinetobacter baumannii* virulence determinants involved in biofilm growth and adherence to host epithelial cells. Virulence. 2016; 7 (4): 367-8.
- Wroblewska MM, Sawicka-Grzelak A, Marchel H, Luczak M, Sivan A. Biofilm production by clinical strains of *Acinetobacter baumannii* isolated from patients hospitalized in two tertiary care hospitals. FEMS Immunol Med Microbiol. 2008; 53 (1): 140-4.
- Falciglia G, Hageman JR, Schreiber M, Alexander K. Antibiotic Therapy and Early Onset Sepsis. NeoReviews. 2012; 13 (2): e86.
- Lopes BS, Amyes SGB. Role of *ISAbal* and *ISAbal25* in governing the expression of *bla_{ADC}* in clinically relevant *Acinetobacter baumannii* strains resistant to cephalosporins. J Med Microbiol. 2012; 61 (8): 1103-8.
- Gu B, Tong M, Zhao W, Liu G, Ning M, Pan S, et al. Prevalence and Characterization of Class I Integrons among *Pseudomonas aeruginosa* and *Acinetobacter baumannii* Isolates from Patients in Nanjing, China. J Clin Microbiol. 2007; 45 (1): 241-3.
- Bou G, Cerveró G, Domínguez MA, Quereda C, Martínez-Beltrán J. Characterization of a Nosocomial Outbreak Caused by a Multiresistant *Acinetobacter baumannii* Strain with a

Carbapenem-Hydrolyzing Enzyme: High-Level Carbapenem Resistance in *A. baumannii* Is Not Due Solely to the Presence of β -Lactamases. *J Clin Microbiol.* 2000; 38 (9): 3299-305.

15. Sutherland IW. The biofilm matrix – an immobilized but dynamic microbial environment. *Trends Microbiol.* 2001;9 (5): 222-7.

16. Stoodley P, Sauer K, Davies DG, Costerton JW. Biofilms as Complex Differentiated Communities. *Annu Rev Microbiol.* 2002; 56 (1): 187-209.

17. De la Fuente-Núñez C, Korolik V, Bains M, Nguyen U, Breidenstein EBM, Horsman S, et al. Inhibition of Bacterial Biofilm Formation and Swarming Motility by a Small Synthetic Cationic Peptide. *Antimicrob Agents Chemother.* 2012; 56 (5): 2696-704.

18. Gaddy JA, Actis LA. Regulation of *Acinetobacter baumannii* biofilm formation. *Future Microbiol.* 2009; 4 (3): 273-8.

19. Bassler BL. How bacteria talk to each other: regulation of gene expression by quorum sensing. *Curr Opin Microbiol.* 1999; 2 (6): 582-7.

20. Goh HMS, Beatson SA, Totsika M, Moriel DG, Phan M-D, Szubert J, et al. Molecular Analysis of the *Acinetobacter baumannii* Biofilm-Associated Protein. *Appl Environ Microbiol.* 2013; 79 (21): 6535-43.

21. Choi AHK, Slamti L, Avci FY, Pier GB, Maira-Litrán T. The *pgaABCD* Locus of *Acinetobacter baumannii* Encodes the Production of Poly- β -1-6-N-Acetylglucosamine, Which Is Critical for Biofilm Formation. *J Clin Microbiol.* 2009; 191 (19): 5953-63.

22. Longo F, Vuotto C, Donelli G. Biofilm formation in *Acinetobacter baumannii*. *New Microbiol.* 2014; 37 (2): 119-27.

23. Dubrovin EV, Popova AV, Kraevskiy SV, Ignatov SG, Ignatyuk TE, Yaminsky IV, et al. Atomic Force Microscopy Analysis of the *Acinetobacter baumannii* Bacteriophage AP22 Lytic Cycle. *PLoS ONE.* 2012; 7 (10): e47348.

24. Soon RL, Nation RL, Harper M, Adler B, Boyce JD, Tan C-H, et al. Effect of colistin exposure and growth phase on the surface properties of live *Acinetobacter baumannii* cells examined by atomic force microscopy. *Int J Antimicrob Agents.* 2011; 38 (6): 493-501.

25. Ghajavand H, Esfahani BN, Havaei SA, Moghim S, Fazeli H. Molecular identification of *Acinetobacter baumannii* isolated from intensive care units and their antimicrobial resistance patterns. *Adv Biomed Res.* 2015; 4: 110.

26. Hudzicki J. Kirby-Bauer disk diffusion susceptibility test protocol: American Society for Microbiology; 2009 [updated 08 December. 1-23]. Available from: <https://www.asmscience.org/content/education/protocol/protocol.3189?crawler=true>.

27. Weinstein MP, Patel JB, Campeau S, Eliopoulos GM, Marcelo MF, Humphries RM, et al. Performance Standards for Antimicrobial Susceptibility Testing M100. 28th ed. USA: Clinical and Laboratory Standards Institute (CLSI); 2018.

28. Jorgensen JH, Ferraro MJ. Antimicrobial susceptibility testing: a review of general principles and contemporary practices. *Clin Infect Dis.* 2009; 49 (11): 1749-55.

Meropenem effects on pgaA and analysis of AFM images

29. Mathur T, Singhal S, Khan S, Upadhyay DJ, Fatma T, Rattan A. Detection of biofilm formation among the clinical isolates of Staphylococci: an evaluation of three different screening methods. *Indian J Med Microbiol.* 2006;24(1):25-9.

30. Nosrati N, Honarmand Jahromy S, Zare Karizi S. Comparison of Tissue Culture Plate, Congo red Agar and Tube Methods for Evaluation of Biofilm Formation among Uropathogenic *E. coli* Isolates. *Iran J Med Microbiol.* 2017; 11 (3): 49-58.

31. Stepanović S, Vuković D, Hola V, Bonaventura GD, Djukić S, Ćirković I, et al. Quantification of biofilm in microtiter plates: overview of testing conditions and practical recommendations for assessment of biofilm production by staphylococci. *APMIS.* 2007; 115 (8): 891-9.

32. Tollersrud T, Berge T, Andersen SR, Lund A. Imaging the surface of *Staphylococcus aureus* by atomic force microscopy. *APMIS.* 2001; 109 (7-8): 541-5.

33. Boudjemaa R, Steenkeste K, Canette A, Briandet R, Fontaine-Aupart M-P, Marlière C. Direct observation of the cell-wall remodeling in adhering *Staphylococcus aureus* 27217: An AFM study supported by SEM and TEM. *Cell Surf.* 2019; 5: 100018.

34. Chao Y, Zhang T. Optimization of fixation methods for observation of bacterial cell morphology and surface ultrastructures by atomic force microscopy. *Appl Microbiol Biotechnol.* 2011; 92 (2): 381-92.

35. Liu BY, Zhang GM, Li XL, Chen H. Effect of glutaraldehyde fixation on bacterial cells observed by atomic force microscopy. *Scanning.* 2012; 34 (1): 6-11.

36. Eales MG, Ferrari E, Goddard AD, Lancaster L, Sanderson P, Miller C. Mechanistic and phenotypic studies of bicarinalin, BP100 and colistin action on *Acinetobacter baumannii*. *Res Microbiol.* 2018; 169 (6): 296-302.

37. Marinho AR, Martins PD, Ditmer EM, d'Azevedo PA, Frazzon J, Sand STVD, et al. Biofilm formation on polystyrene under different temperatures by antibiotic resistant *Enterococcus faecalis* and *Enterococcus faecium* isolated from food. *Braz J Microbiol.* 2013; 44 (2): 423-6.

38. Selasi GN, Nicholas A, Jeon H, Na SH, Kwon HI, Kim YJ, et al. Differences in Biofilm Mass, Expression of Biofilm-Associated Genes, and Resistance to Desiccation between Epidemic and Sporadic Clones of Carbapenem-Resistant *Acinetobacter baumannii* Sequence Type 191. *PLoS ONE.* 2016; 11 (9): e0162576.

39. Clifford RJ, Milillo M, Prestwood J, Quintero R, Zurawski DV, Kwak YI, et al. Detection of Bacterial *16S rRNA* and Identification of Four Clinically Important Bacteria by Real-Time PCR. *PLoS ONE.* 2012; 7 (11): e48558.

40. Nasr P. Genetics, epidemiology, and clinical manifestations of multidrug-resistant *Acinetobacter baumannii*. *J Hosp Infect.* 2020; 104 (1): 4-11.

41. Howard A, O'Donoghue M, Feeney A, Sleator RD. *Acinetobacter baumannii*. *Virulence.* 2012; 3 (3): 243-50.

42. Klevens RM, Edwards JR, Richards CL, Horan TC, Gaynes RP, Pollock DA, et al. Estimating Health Care-Associated Infections and Deaths in U.S. Hospitals, 2002. *Publ Health Rep.* 2007; 122 (2): 160-6.

Najafi

43. Jahangiri S, Malekzadegan Y, Motamedifar M, Hadi N. Virulence genes profile and biofilm formation ability of *Acinetobacter baumannii* strains isolated from inpatients of a tertiary care hospital in southwest of Iran. *Gene Rep.* 2019; 17: 100481.
44. Motbainor H, Bereded F, Mulu W. Multi-drug resistance of blood stream, urinary tract and surgical site nosocomial infections of *Acinetobacter baumannii* and *Pseudomonas aeruginosa* among patients hospitalized at Felegehiwot referral hospital, Northwest Ethiopia: a cross-sectional study. *BMC Infect Dis.* 2020; 20 (1): 92.
45. Afshar Yavari SH, Rota S, Caglar K, Fidan I. DETERMINATION OF RESISTANCE PATTERN OF ISOLATED ACINETOBACTER BAUMANNII FROM INTENSIVE CARE UNITS (ICUS) IN GAZI HOSPITAL, ANKARA. *Nursing and Midwifery Journal* 2016; 13 (10) : 912-918. URL: <http://unmf.umsu.ac.ir/article-1-2772-en.html>.
46. Farsiani H, Mosavat A, Soleimanpour S, Nasab MN, Salimizand H, Jamehdar SA, et al. Limited genetic diversity and extensive antimicrobial resistance in clinical isolates of *Acinetobacter baumannii* in north-east Iran. *J Med Microbiol.* 2015; 64 (7): 767-73.
47. Moradi J, Hashemi FB, Bahador A. Antibiotic Resistance of *Acinetobacter baumannii* in Iran: A Systemic Review of the Published Literature. *Osong Public Health Res Perspect.* 2015; 6 (2): 79-86.
48. Beganovic M, Luther MK, Daffinee KE, LaPlante KL. Biofilm prevention concentrations (BPC) of minocycline compared to polymyxin B, meropenem, and amikacin against *Acinetobacter baumannii*. *Diagn Microbiol Infect Dis.* 2019; 94 (3): 223-6.
49. Wang Y-C, Kuo S-C, Yang Y-S, Lee Y-T, Chiu C-H, Chuang M-F, et al. Individual or Combined Effects of Meropenem, Imipenem, Sulbactam, Colistin, and Tigecycline on Biofilm-Embedded *Acinetobacter baumannii* and Biofilm Architecture. *Antimicrob Agents Chemother.* 2016; 60 (8): 4670-6.
50. Yang C-H, Su P-W, Moi S-H, Chuang L-Y. Biofilm Formation in *Acinetobacter Baumannii*: Genotype-Phenotype Correlation. *Molecules.* 2019; 24 (10): 1849.
51. Perez LRR. *Acinetobacter baumannii* displays inverse relationship between meropenem resistance and biofilm production. *J Chemother.* 2015; 27 (1): 13-6.
52. Bazari PAM, Honarmand Jahromy S, Zare Karizi S. Phenotypic and genotypic characterization of biofilm formation among *Staphylococcus aureus* isolates from clinical specimens, an Atomic Force Microscopic (AFM) study. *Microb Pathog.* 2017; 110: 533-9.
53. Honarmand jahromi S, Noorbakhsh F, Hosseini O, Sajdeh A. Visualization of acidic and alkaline pH effect on biofilm formation of *Staphylococcus aureus* isolates by Atomic force microscope. *Int J Mol Clin Microbiol.* 2018; 8 (1): 942-9.
54. Hatami R. The frequency of multidrug-resistance and extensively drug-resistant *Acinetobacter baumannii* in west of Iran. *J Exp Clin Med.* 2018; 1 (1): 4-8.

Cite this article:

Najafi M.M. Meropenem inhibits *Acinetobacter baumannii* biofilm formation by downregulating *pgaA* gene expression. *J Med Microbiol Infect Dis*, 2023; 11 (2): 86-95. DOI: 10.61186/JoMMID.11.2.86.